ARTICLES

Infrared Chemiluminescence Studies of the H + (CH₃)₃COCl and H + RC(O)SCl (R = Cl, F, OCH₃) Reactions: Observation of OCS Infrared Chemiluminescence

G. C. Manke, II* and D. W. Setser

Department of Chemistry, Kansas State University, Manhattan, Kansas 66506

Received: March 20, 2000; In Final Form: September 26, 2000

Infrared chemiluminescence from a room-temperature flow reactor was used to study the reactions of H atoms with $(CH_3)_3COCl$, $ClC(O)SCl$, $FC(O)SCl$, and $CH_3OC(O)SCl$. Infrared emission spectra were recorded from the HCl, HF, and OCS products. The anharmonic shifts from bands involving v_1, v_2, and v_3 excitation are too small to obtain information about bending vs stretch excitation of OCS from the $\Delta v_3 = -1$ spectra; however, a computer simulation method was developed to analyze the $\Delta v_3 = -1$ transition to assign the average total vibrational energy of OCS, $\langle E_v(OCS) \rangle$. The enthalpy changes for the carbonylsulfenyl chloride reactions were estimated from ab initio calculations. The proposed mechanism for the carbonylsulfenyl chlorides includes two reaction pathways: one involves interaction with the S−Cl bond to give HCl; the second involves an RC(O)SCl·H adduct that subsequently gives RH and OCS (+Cl). The $\langle E_v(OCS) \rangle$ values were 17.2, 14.6, and 8.4 kcal mol^{-1} from $FC(O)SCl$, $CH_3OC(O)SCl$, and $ClC(O)SCl$, respectively. The fraction of the available energy released as HCl vibrational energy, $\langle f_V(HCl) \rangle$, from reaction with the S−Cl bond was ~0.3 for all three reactions. The reaction mechanism for H + $(CH_3)_3COCl$, which was employed as a reference reaction, is thought to be direct abstraction and $\langle f_V(HCl) \rangle$ is 0.23.

I. Introduction

The infrared chemiluminescence (IRCL) technique is an established method to measure vibrational, and even rotational, product state distributions and rate constants from reactions giving HX products (X = O, F, Cl, Br).[1,2] This laboratory has employed infrared emission from a flow reactor to characterize the reaction kinetics and the vibrational distributions of many primary and secondary reactions involving both uni- and bimolecular elementary steps giving HX products. More recently, the flow reactor technique was extended to observe infrared spectra from triatomic product molecules, including H_2O, HOD, D_2O,[3-5] CO_2,[3a] HNO,[6] HCN, and HNC.[7] The vibrational distributions for the molecules just mentioned were assigned by computer simulation of the spectra obtained at experimental conditions that were chosen to avoid vibrational relaxation. By taking advantage of anharmonic shifts, the assignment of specific vibrational distributions to bend and stretch modes from the strongest emission band, e.g., $\Delta v_3 = -1$ for CO_2,[3a] generally was possible. One of the major goals of the present work was to examine the IRCL technique for reactions that give OCS as a product. The large Einstein emission coefficient ($A = 385$ s^{-1})[8] for the asymmetric stretch mode, $v_3 = 2071$ cm^{-1}, makes OCS a favorable candidate. Unfortunately, the modest, and similar, anharmonicity constants,[9] $\chi_{13} = -6.46$ cm^{-1}, $\chi_{22} = -7.55$ cm^{-1}, and $\chi_{33} = -11.46$ cm^{-1}, make assignment of the $\Delta v_3 = -1$ spectra to specific

bend−stretch distributions impossible, even by computer simulation. An additional problem for OCS is the close energy match among several vibrational levels and the expected rapid equilibration of bend−stretch levels of a similar energy.[10,11] For these reasons, only the average total energy and the general shape of the vibrational distribution can be deduced from the observed $\Delta v_3 = -1$ spectra. As far as we know, the only other report of IRCL from OCS has been from the O + CS_2 reaction.[12] However, the emission was not consistently observed[12] and the main products are CS + SO.

The H + carbonylsulfenyl chloride reactions were selected as chemical systems that might give OCS as a product. By analogy to H + RSCl[13] and ROCl[14,15] reactions, we anticipated rapid abstraction of a Cl atom followed by decomposition of the RC(O)S radical (as for HCO_2)[16] or a secondary reaction of H atoms with RC(O)S followed by HR elimination with concomitant formation of OCS. The H + $ClC(O)SCl$, $FC(O)SCl$, and $CH_3OC(O)SCl$ reactions were examined, and infrared emission was observed from the HCl, HF, and OCS products. For purposes of comparison, we also studied the H + $(CH_3)_3$-COCl reaction, which proceeds via direct Cl atom abstraction. Direct Cl atom abstraction reactions[14,15] normally give inverted distributions with $\langle f_V(HCl) \rangle \approx 0.3$, whereas unimolecular HCl elimination processes give $\langle f_V(HCl) \rangle \leq 0.2$ and noninverted distributions.[17-19]

The principal experimental data are the HCl($\Delta v = -1$), HF($\Delta v = -1$), and OCS($\Delta v_3 = -1$) infrared emission spectra from which vibrational distributions and relative product concentrations are deduced. The room-temperature rate constants

* To whom correspondence should be addressed. Current address: Bldg. 619, AFRL/DELC, 3500 Aberdeen Ave. SE, Kirtland AFB, NM 87117-5776.

for HX production also were measured by comparison to the H + Cl$_2$ reaction, and the rate constants for HCl (or HCl + HF) formation are: $(3.0 \pm 1.0) \times 10^{-12}$, $\sim 1 \times 10^{-12}$, and $\sim 1.7 \times 10^{-12}$ cm^3 molecule^{-1} s^{-1} for R = CH$_3$O, Cl, and F, respectively. The total H atom removal rate constant by ClC(O)SCl was $(3.7 \pm 0.5) \times 10^{-12}$ cm^3 molecule^{-1} s^{-1}, indicating the possible presence of one or more dark reactions. The primary reaction mechanism for the carbonylsulfenyl chlorides appears to be a combination of addition and abstraction processes. The addition step occurs at either the O or S position (although the C position cannot be entirely ruled out), and it is followed by HR (or HCl) elimination:

$$H + R-C(O)S-Cl \rightarrow HCl + R-C(O)S \quad (1a)$$

$$R-C(O)S \rightarrow R + OCS \quad (1b)$$

$$H + R-C(O)S-Cl \rightarrow [R-C(O)S-Cl\cdot H] \quad (2a)$$

$$[R-C(O)S-Cl\cdot H] \rightarrow R-C(O)SH + Cl \quad (2b.1)$$

$$\rightarrow R-C(O)S + HCl \quad (2b.2)$$

$$\rightarrow OCS-Cl + HR \quad (2b.3)$$

$$OCS-Cl \rightarrow OCS + Cl \quad (2c)$$

We found no evidence to support a secondary reaction of H atoms with RC(O)S as the *major* source of OCS emission. The direct abstraction of Cl atom from sulfur (eq 1a) and the addition–elimination step (eq 2b.2) both can lead to HCl emission. The OCS emission can arise from either the direct (eq 1b) or addition (eq 2c) pathways. Since the ΔH_f^o(RC(O)-SCl) are not available, the thermochemistry of these reactions was analyzed using ab initio calculations plus standard thermochemical methods. An upper limit measurement also was made for the S–Cl bond energy from the short wavelength limit of the XeCl(B–X) fluorescence from reactions of CH$_3$OC(O)SCl and ClC(O)SCl with excited-state xenon atoms. A few survey experiments were done with the F + CH$_3$C(O)SH reaction to investigate the possibility of formation of OCS from decomposition of the CH$_3$C(O)S radical.

II. Experimental Methods

II.A. The Flow Reactor. The 0.5-m long, 4.0-cm i.d. Pyrex reactor used in this study already has been described.[3-7] The total Ar flow (typically 4.8 mmol s^{-1}) was monitored with a calibrated Hastings flow meter and directed to various inlet ports of the reactor by needle valves. Tank grade Ar was purified by passage through 3 molecular sieve-filled traps cooled to 195 K. A gate valve separating the reactor from the Roots blower and mechanical pump could be partly closed to reduce the flow velocity; the operating pressure range was 0.3–2.0 Torr. The hydrogen flow was introduced at the entrance of the reactor and the reagent was introduced via a four-jet inlet placed just upstream of the NaCl observation window, which was located 40 cm from the entrance of the reactor. The reaction time, Δt, could be changed from 0.2–1.2 ms by the throttling valve. The H$_2$ flow was passed through a microwave discharge to produce H atoms; the dissociation efficiency has been measured on several occasions[14,15] to be $\sim$50%. Reagent gases, except for CH$_3$OC(O)SCl, were stored in darkened Pyrex bulbs as 10% mixtures in argon, and their flow rates were regulated by a Teflon needle valve and measured by the pressure rise in calibrated volumes. Methoxycarbonylsulfenyl chloride has a

vapor pressure of 8 Torr at room temperature, and a flow of Ar was passed over the surface of the liquid maintained at 0 °C to introduce CH$_3$OC(O)SCl into the reactor. The flow rate was determined by collecting CH$_3$OC(O)SCl in a liquid-nitrogen-cooled trap and weighing the contents of the trap.
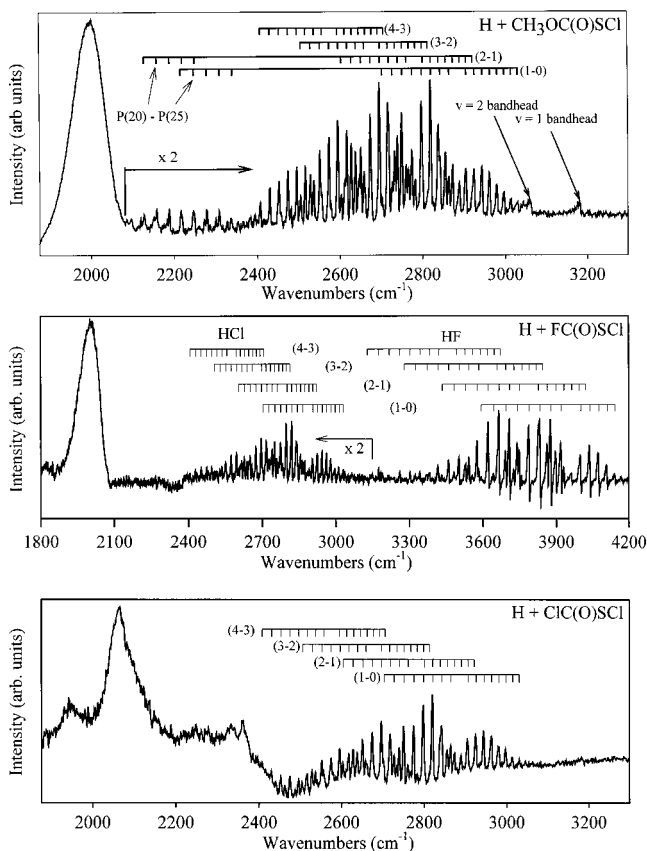
Experiments were performed with one reagent concentration held constant while the other was varied. For example, constant [H] was maintained, usually 8.0×10^{12} cm^{-3} for H + CH$_3$OC(O)SCl and 2.0×10^{13} for H + ClC(O)SCl and FC(O)SCl, while [RC(O)SCl] was varied from 0.5 to 2.0×10^{13} cm^{-3}. Alternatively, [RC(O)SCl] was held constant, typically $0.7–1.0 \times 10^{13}$ cm^{-3}, while [H] was varied from 0.5 to 3.0×10^{13} cm^{-3}.

Methoxycarbonylsulfenyl chloride, ClC(O)SCl, and (CH$_3$)$_3$-COCl were purchased (98% or better purity) from either Aldrich or TCI America and loaded into the reservoirs after degassing by a single distillation step. Fluorocarbonylsulfenyl chloride was synthesized by the reaction of ClC(O)SCl with SbF$_3$ in tetrahydrothiophene dioxide.[20] Several distillations were required to separate pure FC(O)SCl from the solvent and ClC(O)SCl. Infrared absorption spectra confirmed the presence of FC(O)SCl and the absence of ClC(O)SCl. The H + Cl$_2$ reaction was used as a reference reaction for rate constant measurements; the research grade Cl$_2$ was purchased from Matheson.

Infrared emission from the reactor was collected through NaCl windows by a backing mirror plus a 5-cm focal length CaF$_2$ lens and focused into a BioRad Fourier transform infrared spectrometer (FTIR). The instrument used a liquid-nitrogen-cooled InSb detector (Infrared Associates Inc., $D^* = 2.165 \times 10^{11}$ cm Hz$^{0.5}$ W^{-1}), which has a cold filter to block radiation below $\sim$1850 cm^{-1}. Each emission spectrum was acquired by subtracting a thermal background spectrum from the experimental spectrum. The difference spectrum is very sensitive to the background spectrum near the 1850 cm^{-1} cutoff. The OCS emission is also in this region, and care must be exercised to acquire a suitable background spectrum. All spectra were collected with 2 cm^{-1} resolution and corrected for the wavelength response of the detector which is approximately 5 times more sensitive for OCS than for HCl emission. The CH$_3$OC-(O)SCl reaction gave the most intense emission of the RC(O)-SCl molecules, and a characteristic spectrum is shown in Figure 1 for a pressure of 0.3 Torr and a reaction time of 0.3 ms. The major part of the HCl spectrum extends from 3200 to 2400 cm^{-1} and the strong chemiluminescence in the 1900–2100 cm^{-1} range is the OCS($\Delta \nu_3 = -1$) emission. The weak features in the 2400–2100 cm^{-1} range are P branch lines from $J \geq 10$ levels of HCl($v = 1, 2$); the R branch bandheads at 3050 and 3175 cm^{-1} also are from these high J levels. These small populations are the residue of the nascent rotational distribution, which must have been highly rotationally excited.[13,21] Emission was observed from HF, HCl, and OCS from the FC(O)SCl reaction, and the shapes of some of the HF lines are not ideal (see Figure 1). This is a consequence of a poor choice for the phase factor by the FT software. Reliable relative HF$_{v,J}$ concentrations were obtained, as deduced from either its P or R branch lines, when the peak height was measured from the minimum point below the baseline to the top of the peak of the distorted lines.

II.B. Data Analysis. The relative concentrations of HCl or HF can be calculated from the area of each vibrational–rotational line from a rotationally resolved spectrum:

$$[HX(v \geq 1)] = \sum_v \sum_J \frac{\text{area}(v,J)}{A_{v,J} R(\omega)} \quad (3)$$

Observation of OCS Infrared Chemiluminescence

J. Phys. Chem. A, Vol. 104, No. 47, 2000 **11015**

Figure 1. Emission spectra from the H + $CH_3OC(O)SCl$, FC(O)SCl, and ClC(O)SCl reactions for Δt = 0.3, 0.6, and 0.3 ms and pressure = 0.3, 2.0, and 1.0 Torr, respectively. The strong band at $1900-2100$ cm^{-1} is the $\Delta \nu_3 = -1$ emission of OCS. The emission from high J levels of HCl(ν = 1 and 2) from the H + $CH_3OC(O)SCl$ reaction is labeled in both the P and R branches. These spectra have not been corrected for detector response, which increases by a factor of ~ 2 from 4100 to 3000 cm^{-1} and by another factor of ~ 5 from 3000 to 2000 cm^{-1}. The weaker signal from the ClC(O)SCl reaction illustrates its slower reaction rate. Note the scale changes at ~ 2100 cm^{-1} for $CH_3OC(O)SCl$ and 3200 cm^{-1} for FC(O)SCl.

The area(ν,J) is the product of the peak height and $\Delta\omega$, where $\Delta\omega$ is the half-width and both P and R branch areas are needed; $R(\omega)$ is the detector response function. The majority of the rotational distribution is in the 300 K Boltzmann component, and we normally found the relative vibrational distribution, P_ν, as described below and then summed over the ν levels to obtain relative HX($\nu \geq 1$) concentrations. The P_ν values for HF or HCl were calculated by dividing the response corrected peak height by $A_{\nu,J}$ and the Boltzmann fraction in level J for all nonoverlapped rotational lines from a given ν level. These numbers were averaged to give P_ν. This procedure was repeated for each ν level to get a relative distribution. The total relative HX concentration was obtained by including P_0 from an empirical estimate for the HX(ν = 0) contribution based on the P_1-P_4 distribution. The $\Delta\nu = -1$ Einstein coefficients[22] of HCl for ν = 1–4 are 40, 70, 90, and 100 s^{-1}, and those for HF are 195, 334, 423, and 467 s^{-1}.

The observed OCS emission may be described by the overlap of the transitions with $\Delta\nu_3 = -1$ with combination and hot bands: $(\nu_1, \nu_2^l, \nu_3) - (\nu_1, \nu_2^l, \nu_3 - 1)$. The band centers were calculated using the conventional formula for the vibrational energy levels:[9]

$$G(\nu_1,\nu_2^l,\nu_3) = \sum_i \omega_i\left(\nu_i + \frac{d_i}{2}\right) + \sum_i \sum_{k \geq i} \chi_{ik}\left(\nu_i + \frac{d_i}{2}\right)\left(\nu_k + \frac{d_k}{2}\right) +$$
$$\chi_{ll}l^2 + \sum_i \sum_{j \geq i} \sum_{k \geq j} y_{ijk}\left(\nu_i + \frac{d_i}{2}\right)\left(\nu_j + \frac{d_j}{2}\right)\left(\nu_k + \frac{d_k}{2}\right) \quad (4)$$

where d_i is the degeneracy of the vibration ν_i ($d_1 = d_3 = 1$, $d_2 = 2$), and l is the vibrational angular momentum due to the degeneracy of the bending vibration ν_2. The frequencies, ω_i, anharmonicity coefficients, χ_{ik}, and g_{22} coefficient were taken from the literature.[9] For simplicity, the third-order terms with anharmonicity constants, y_{ijk}, were truncated. The rotational line positions for $\Sigma-\Sigma$ transitions ($l = 0$ both in the upper and lower state) were given by:

$$E_{v,J} = G(\nu_1,\nu_2^l,\nu_3) + (B' + B'')m + (B' - B'')m^2 \quad (5)$$

where $m = J + 1$ for the R branch and $m = -J$ for the P branch. In the bands with $l \neq 0$ ($\Pi-\Pi$, $\Delta-\Delta$, ...), the Q branch was added for which:

$$E_{v,J} = G(\nu_1,\nu_2^l,\nu_3) + (B' - B'')J + (B' - B'')J^2 \quad (6)$$

In the formula for the line positions, B' and B'' are the rotational constants in the upper and lower vibrational state, equal to:

$$B_v = B_e - \sum_i \alpha_i\left(\nu_i + \frac{d_i}{2}\right) + \sum_{j \geq i} \gamma_{ij}\left(\nu_i + \frac{d_i}{2}\right)\left(\nu_j + \frac{d_j}{2}\right) \quad (7)$$

Rotational constants B_e = 0.203457 cm^{-1}, α_1 = 66.9499 × 10^{-5} cm^{-1}, α_2 = −33.8966 × 10^{-5} cm^{-1}, and α_3 = 124.959 × 10^{-5} cm^{-1} were taken from ref 9. Einstein emission coefficients for the relative intensities of individual rotational lines were calculated by the expression:

$$I \propto \nu^3(2J + 1) \exp(-B'J(J + 1)/kT)S_{IJ}S_v \quad (8)$$

where S_{IJ} is the rotational line intensity or Hönl−London factor and S_v is the square of the rotationless transition moment, which is equal[8] to 0.374 D for ν_3 = 1. The Einstein coefficients were assumed to scale with ν_3 according to the harmonic oscillator approximation, but to be independent of ν_1 and ν_2.

The P and R branch rotational lines are separated by only 0.4 cm^{-1}, and each line was given a width corresponding to the spectrometer resolution and co-added to simulate a spectral band. Calculated spectra from the (2,0,1), (0,2,1), (0,4,1), and (0,8,1) levels are shown in Figure 2. The $\Delta\nu_3 = -1$ spectra do shift to smaller wavenumbers with increasing vibrational energy, but a spectrum cannot be assigned to a specific (ν_1,ν_2,ν_3) distribution because the bands from several OCS($\nu_1,\nu_2,1$) levels are overlapped.

Strong, and resolved, Q branch features from highly excited CO_2 bending levels were the key to assigning the distribution from the $\Delta\nu_3 = -1$ spectra from the decomposition of acetic acid.[3a] Although Q branch structure is evident in the calculated spectra form high ν_2 levels (see Figure 2), the experimental OCS spectra do not show resolved Q branches. Bending excitation of OCS is expected, since all of the expected precursor radicals have a bent structure. Because of the nearly commensurate nature of the ν_1(859 cm^{-1}), ν_2(520 cm^{-1}), and ν_3(2071 cm^{-1}) frequencies, numerous near energy resonances exist. The vibrational relaxation rates[10,11] suggest that nearly isoenergetic vibrational levels of OCS will tend to equilibrate in 0.4 ms at 1 Torr Ar. Because of the expected collisional mixing of
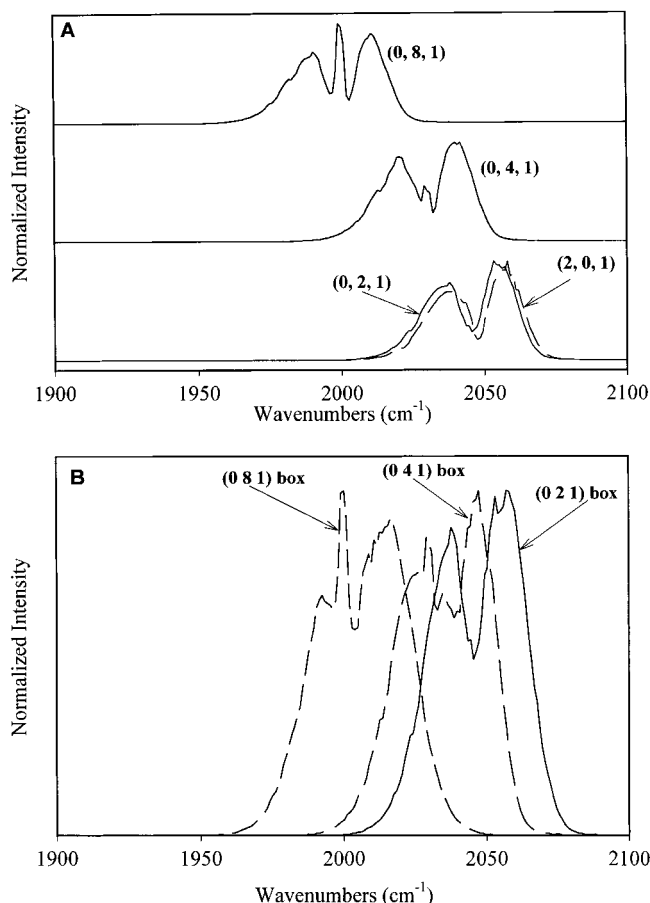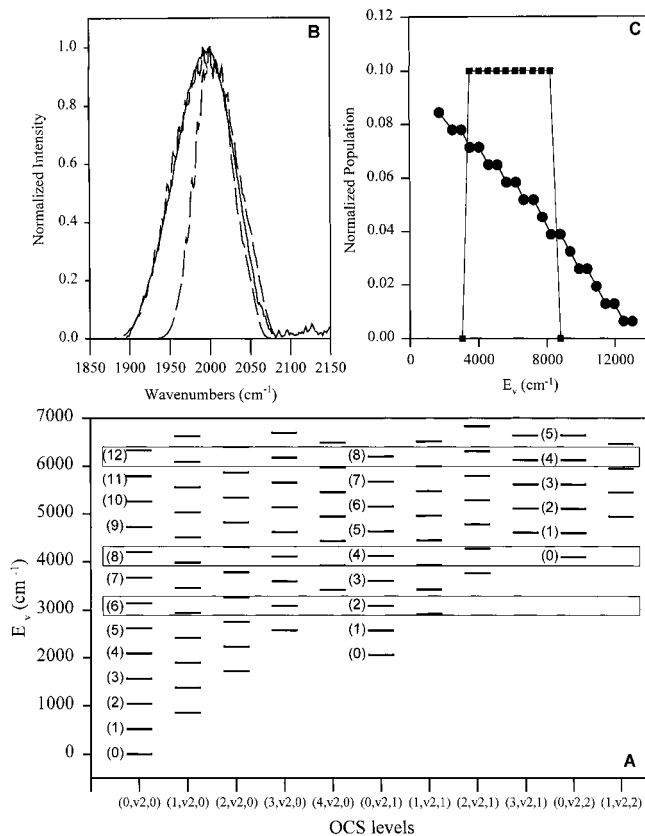
Figure 2. (A) Calculated $\Delta v_3 = -1$ spectra from four vibrational levels of OCS at 2 cm^{-1} resolution. Note the Q branch in the (0,8,1) band. (B) Calculated OCS basis spectra from the (0,8,1), (0,4,1), and (0,2,1) energy boxes with normalization to the same height of the strongest feature of each spectrum.

Figure 3. (A) Schematic presentation of the vibrational levels of OCS. The division of the levels into boxes (see text) is illustrated for the (0,2,1), (0,4,1), and (0,8,1) boxes. (B) Simulations of the $\Delta v_3 = -1$ OCS emission spectrum from the H + CH$_3$OC(O)SCl reaction for the two vibrational distributions shown in panel C. The flat distribution gives the narrower emission spectrum.

**TABLE 1: Summary of OCS(v_1,v_2,v_3) Energy Box Description**

box^{a,b}	emitting fraction^b	average Einstein coeff (s^{-1})^c	$\langle E_b \rangle$ cm^{-1}
(0 0 1)	0.08	385	2000
(0 1 1)	0.11	385	2525
(0 2 1)	0.22	385	3037
(0 3 1)	0.28	385	3527
(0 4 1)	0.31	415	4060
(0 5 1)	0.41	428	4606
(0 6 1)	0.39	397	5126
(0 7 1)	0.45	454	5640
(0 8 1)	0.34	565	6185
(0 9 1)	0.38	576	6640
(0 10 1)	0.46	595	7224
(0 11 1)	0.52	618	7734
(0 12 1)	0.57	660	8239
(0 13 1)	0.53	599	8784
(0 14 1)	0.60	601	9358
(0 15 1)	0.65	646	9886
(0 16 1)	0.68	663	10355
(0 17 1)	0.67	739	10901
(0 18 1)	0.69	752	11444
(0 19 1)	0.67	816	11967
(0 20 1)	0.69	875	12519
(0 21 1)	0.66	830	13048

^{a} The six energy levels below (0,0,1) are not included in this table. ^{b} See Figure 2 for a listing of levels below 7000 cm^{-1}. ^{c} The Einstein coefficients were assumed to scale with v_3 according to the harmonic oscillator approximation but to be independent of v_2 and v_1.

(v_1,v_2,v_3) populations of the same total energy, the energy range was divided into boxes, with each (0,v_2,1) bending level defining the center of a box and extending ±200 cm^{-1}. The vibrational levels and the boxes up to 7000 cm^{-1} are illustrated in Figure 3; emission can arise from $v_3 \geq 2$, as well as from $v_3 = 1$ for the ($v_1,v_2 \geq 4$,1) boxes. A basis spectrum from each box was generated for the purpose of simulating experimental spectra. The statistical weight of each (v_1,v_2',v_3) level within a box, relative to the (0,v_2,1) level, was calculated according to eq 9 with $T_{vib} = 300$ K:

$$\frac{N_1}{N_0} = \frac{g_1}{g_0}\exp[-(E_1 - E_0)/kT] \qquad (9)$$

where N_0, N_1, g_0, g_1, E_0, and E_1 are the concentrations, degeneracies, and vibrational energies of the OCS(0,v_2,1) and OCS(v_1,v_2',v_3) levels, respectively, in a box. For example, the (0,4,1) box has four radiating states [(0,4,1), (1,2,1), (2,1,1), (0,0,2)] and six dark states [(0,8,0), (1,6,0), (2,4,0), (3,3,0), (4,1,0), (5,0,0)]. The populations for the (1,2,1), (2,1,1), (0,0,2), and (0,4,1) levels are 0.16, 0.02, 0.02, and 0.11, respectively, and the remaining population is in the dark states. The spectra from each of the four emitting levels were co-added with their relative weights and with the appropriate Einstein coefficients to form the basis spectrum of the (0,4,1) box, which is shown in the lower panel of Figure 2. The weighted energies of all levels in a box were combined to give the average vibrational energy, $E(b)_i$, of a box. Table 1 lists the average Einstein coefficients ($\bar{A}_i$), $E(b)_i$, and the fraction of emitting levels for the "boxes". Basis spectra are all normalized to unity. The assumptions are that levels within each box are equilibrated with

Observation of OCS Infrared Chemiluminescence

J. Phys. Chem. A, Vol. 104, No. 47, 2000 **11017**
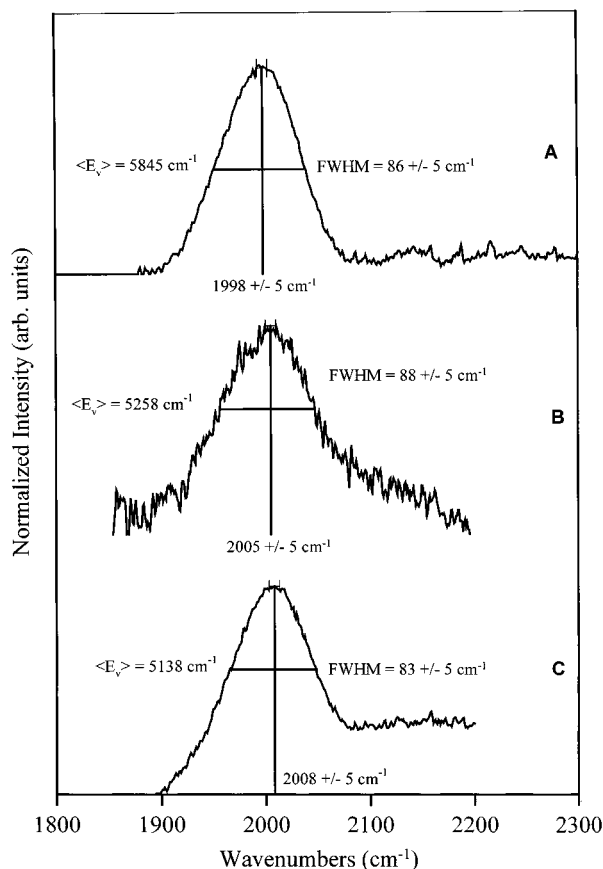
Figure 4. Three representative OCS emission spectra from the H + CH$_3$OC(O)SCl reaction showing the reproducibility for nominally identical conditions (A) and (B) at 0.5 Torr and the small effect of increased pressure (C) at 0.8 Torr. The spectrum in panel C also was chosen to illustrate the necessity of obtaining a satisfactory thermal background spectrum for subtraction.

a temperature of 300 K but that relaxation between boxes are negligible are somewhat arbitrary. The model was chosen to reflect the expectation that nearly isoenergetic vibrational levels will be partly equilibrated. Experimental justification of the model is that the spectra did not change significantly from 0.4 to 0.8 Torr of Ar and the absence of Q branch structure from high v_2 level excitation. The spectra did change at higher pressure (or longer reaction times), vide infra, as expected from loss of total vibrational energy of OCS.

The basis spectra from each box were co-added with appropriate weights to fit a given experimental spectrum. The relative intensities from each box, I_i, are obtained from eq 10:

$$I_i = P_i f_i(e) \bar{A}_i \qquad (10)$$

where P_i is the relative contribution of the ith box to the total distribution and $f_i(e)$ is the fraction of levels that radiate. The relative contributions from each box were changed until a satisfactory visual fit to an experimental spectrum was achieved. The average vibrational energy for the distribution above the OCS(0,0,1) level is given by eq 11:

$$\langle E_v(OCS) \rangle = \sum_i P_i E(b)_i \qquad (11)$$

In computing the global average vibrational energy, the six levels below the energy of the (0,0,1) box must be included. These six levels were considered as one additional box with an average energy of 3.4 kcal mol^{-1}, and the relative contribution

was obtained by extrapolation of the fitted box distribution. A calculated OCS spectrum from the H + CH$_3$OC(O)SCl reaction is shown in Figure 3B for a distribution that monotonically declines with an average energy of 5691 cm^{-1} (Figure 3C). The overall shape and width of the spectrum is matched, but the simulation has slightly more structure (due to Q branches from the high bending levels) than the experimental spectrum, which suggests that our model may still slightly overestimate the contribution from the bending levels. While this distribution is not unique, a flat distribution (Figure 3C) with nearly the same average energy (5898 cm^{-1}) does not fit the experimental spectrum, as shown in Figure 3B. Thus, we conclude that simulation of the $\Delta v_3 = -1$ spectra can provide $\langle E_v(OCS) \rangle$ and the general shape of the distribution.

It is difficult to assign an uncertainty to the calculated $\langle E_v(OCS) \rangle$. Fits to spectra from nominally identical experiments for the CH$_3$OC(O)SCl reaction gave uncertainties of ±200 cm^{-1}. The most serious experimental problem is the proximity to the cutoff limit of the detector and the associated poor baseline for some spectra from background subtraction; see the three spectra shown in Figure 4. However, the model adopted for the simulation probably introduces the largest uncertainty for $\langle E_v(OCS) \rangle$. We first attempted simulations using just the (0,v_2,1) levels of OCS. These simulations showed too much structure from Q branches, and it was necessary to use contributions from (0,v_2,2) or (v_1,v_2,1) levels of a similar energy but with reduced v_2 excitation. Such simulations gave nearly the same average energy as the model that finally was adopted.[23]

The possible loss of vibrational energy by downward relaxation from adjacent boxes must be considered. Three spectra from the CH$_3$OC(O)SCl reaction are shown in Figure 4 that were obtained with pressures of 0.5 or 0.8 Torr and $\Delta t = 0.25 \pm 0.05$ ms. The band center does slightly shift and the bandwidth is narrower in the 0.8 Torr spectrum. A small reduction in the $\langle E_v(OCS) \rangle$ is noticeable at 0.8 Torr, although the trend is barely outside the ±200 cm^{-1} statistical uncertainty. The spectra for reaction times longer than 0.3 ms or pressures higher than 0.8 Torr gave $\langle E_v(OCS) \rangle$ values that were significantly reduced.[23]

In addition to the average vibrational energies, we also wish to compare the relative concentrations of HF, HCl and OCS from intensities measured in the same spectrum. For OCS, the response-corrected total area is related to the total number of emitting molecules:

$$\text{total corrected area} \propto \sum_i N_i \bar{A}_i f_i(e) \qquad (12)$$

The relative concentration of OCS is the sum, $N_{tot} = \sum_i N_i$. Equation 12 can be rewritten in terms of N$_1$, the concentration for the first box (0,0,1), and x_i, which is the ratio N_i/N_1:

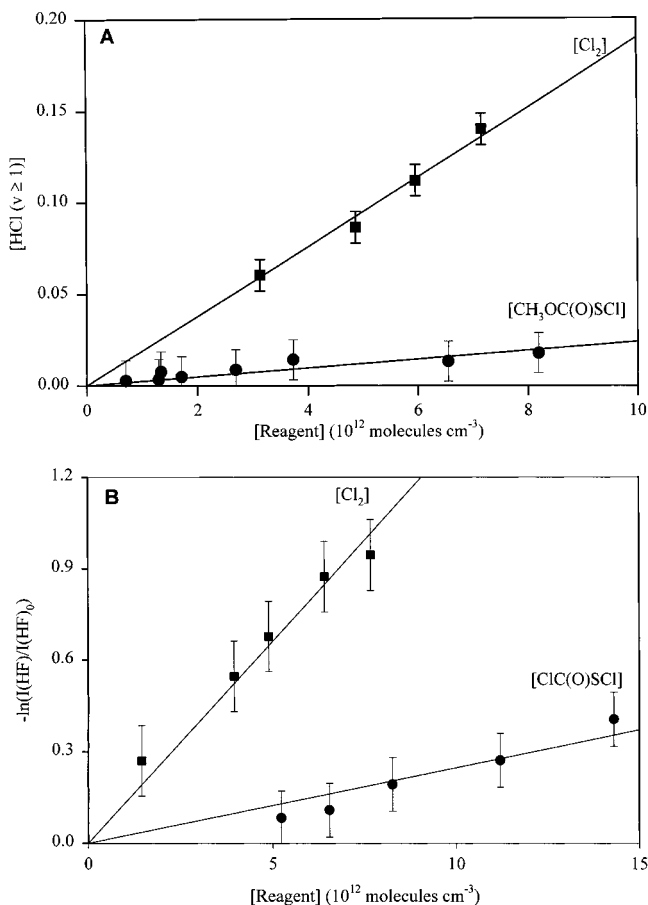$$N_1 \propto \frac{\text{total corrected area}}{\sum_i x_i \bar{A}_i f_i(e)} \qquad (13)$$

and

$$N_{tot} = N_1 \sum_i x_i \qquad (14)$$

Scaling the N_1 value by the sum of x_i gives the OCS concentration in terms of the total band area.

III. Results

III.A. Rate Constants and Relative Product Concentrations. *III.A.1. CH$_3$OC(O)SCl.* This reaction could be studied

Figure 5. Experimental kinetic data from the H + CH$_3$OC(O)SCl and ClC(O)SCl reactions: (A) plot of [HCl($v \geq 0$)] vs [Cl$_2$] and [CH$_3$OC-(O)SCl] for differential rate law conditions ($\Delta t = 0.3$ ms, $P = 0.5$ Torr, and [H] = 8.0×10^{12} cm^{-3}); (B) plot of ln [H] vs [Cl$_2$] and [ClC(O)SCl] for integrated pseudo-first-order rate law conditions. The reaction time corresponds to 4 ms for plug flow approximation to the flow conditions. The relative [H] was monitored from the HF emission intensity arising from the H + F$_2$ reaction; see text for the experimental description.

for short Δt and with [H] and [CH$_3$OC(O)SCl] low enough that relaxation of HCl(v) was not serious. The differential rate law was used to examine the dependence of each product on [H] and [CH$_3$OC(O)SCl]. The data of Figure 5A demonstrate the first-order dependence of [HCl($v \geq 1$)] on [CH$_3$OC(O)SCl] for $\Delta t = 0.24$ ms and [H] = 8.0×10^{12} molecules cm^{-3}. Similar data[23] show that [OCS] formation also was first-order with respect to [CH$_3$OC(O)SCl], [H], and Δt. The HCl($v \geq 1$) formation rate constant, relative to H + Cl$_2$, was obtained as 2.6×10^{-12} cm^3 s^{-1} from the ratio (7.8) of the slopes of the plots in Figure 5A and the recommended value (2.06×10^{-11} cm^3 s^{-1}) for k(H + Cl$_2$).[24] Adjustment for the unobserved molecules in $v = 0$ ($P_0 = P_1 = 0.25$), see section III.B.1, increases [HCl] by a factor of 1.25, and since P_0 from H + Cl$_2$ is negligible, the rate constant for HCl($v \geq 0$) formation is 3.4×10^{-12} cm^3 s^{-1}. This rate constant corresponds to the sum of eqs 1a and 2b.2. Based on three such experiments, the rate constant for HCl($v \geq 0$) formation is $(3 \pm 1) \times 10^{-12}$ cm^3 s^{-1}.

The product intensity ratio adjusted for response, $I_{OCS}/I_{HCl(v \geq 1)}$ was 2.3 ± 0.9 and, within the experimental uncertainty, independent of [H], [CH$_3$OC(O)SCl], and Δt. The kinetic data imply that OCS formation is a primary reaction. After adjustment for the difference in Einstein coefficients and inclusion of HCl($v = 0$), the intensity ratio gives a concentration ratio of [HCl($v \geq 0$)]/[OCS] = 9.9 ± 3.6. Estimation of the contribution

from the OCS levels below the first box as 0.1, see section III.B.1, gives [HCl]/[OCS] = 9.0.

III.A.2. ClC(O)SCl. The emission from this reaction was the weakest of the three RC(O)SCl reactions, and high H atom and ClC(O)SCl concentrations were necessary to collect spectra with acceptable signal-to-noise ratios. A spectrum is shown in Figure 1 for [ClC(O)SCl] = 1.6×10^{13}, [H] = 3.0×10^{13} cm^{-3}, and $\Delta t = 0.3$ ms. The formation of HCl and OCS products were first-order with respect to [ClC(O)SCl] according to tests for the differential rate law. Based on intensity measurements relative to H + Cl$_2$, the rate constant for HCl($v \geq 0$) formation is $\approx 1 \times 10^{-12}$ cm^3 molecules^{-1} s^{-1}. These HCl spectra data had poor signal-to-noise ratios, and this rate constant is uncertain to a factor of 2. The $I_{OCS}/I_{HCl(v \geq 1)}$ ratio was 2.4 ± 0.9, which corresponds to an average [HCl($v \geq 0$)]:[OCS] ratio of 7.6 ± 2.1. Inclusion of the estimate (25%) for the contribution of the lowest six levels of OCS reduces the [HCl]/[OCS] ratio to 6.1.

The total rate constant for H atom removal was measured using the integrated rate law for pseudo-first-order kinetics: e.g. [ClC(O)SCl] > [H]. The relative [H] at the observation window was measured by monitoring the relative HF($\Delta v = -1$) chemiluminescence generated by adding F$_2$ at the reagent inlet. The ClC(O)SCl or Cl$_2$ reagent was added at the entrance to the flow reactor; the total reaction time was ~ 4 ms according to the plug-flow approximation with ideal mixing. The HF($\Delta v = -1$) signal was reduced as [Cl$_2$] or [ClC(O)SCl] was increased, as shown in Figure 5B. The ratio of the slopes of the plots in Figure 5B is 5.2 ± 0.7. This ratio can be used to obtain a rate constant of $(3.7 \pm 0.5) \times 10^{-12}$ cm^3 s^{-1} for removal of H atom by ClC(O)SCl; the actual reaction time cancels from the ratio. The difference of 3.7 between the HCl($v \geq 0$) formation rate constant and the total H atom removal rate constant is considered significant, and other reaction channels may exist that consume H and do not give chemiluminescence. However, secondary reactions involving radicals also may consume some H atoms.

III.A.3. FC(O)SCl. Plots of [HF($v \geq 1$)], [HCl($v \geq 1$)], and [OCS($v_3 \geq 1$)] vs [FC(O)SCl] at constant [H] and vs [H] at constant [FC(O)SCl] were consistent with a first-order dependence of these products on the H and FC(O)SCl concentrations.[23] The HCl emission was weak, see Figure 1; however, after adjustment for Einstein coefficients the [HF($v \geq 0$)]/[HCl($v \geq 0$)] ratio was equal to 0.47 ± 0.11 for a range of conditions. The stronger HF(v) emission was used to estimate the HF formation rate constants by comparison of [HF($v \geq 1$)] to the [HCl($v \geq 1$)] from H + Cl$_2$ in a plot like Figure 5A. The HF($v \geq 1$) formation rate constant is 4.1×10^{-13} cm^3 s^{-1}. The P_0:P_1 ratio was estimated as 0.9, and k(HF($v \geq 0$)) is 5.4×10^{-13} cm^3 s^{-1}. Since the [HF($v \geq 0$)]:[HCl($v \geq 0$)] ratio is 0.47, the total rate for [HX($v \geq 0$)] formation is $\sim 1.7 \times 10^{-12}$ cm^3 s^{-1}; the estimated uncertainty was assigned as a factor of 2 largely because the lack of sample limited the number of experiments. The average I_{HF}/I_{OCS} and I_{HCl}/I_{OCS} ratios were 2.5 ± 0.8 and 0.95 ± 0.16, respectively. Converting these numbers to concentration ratios gave [HF($v \geq 0$)]/[OCS] = 2.5 ± 0.9 and [HCl($v \geq 0$)]/[OCS] = 4.8 ± 0.9; assignment of a 10% contribution to OCS levels below the first box, see section III.B.3, lowered these ratios to 2.3 and 4.4.

III.A.4. (CH$_3$)$_3$COCl. Even for the fastest pumping speed and low [H], a strong HCl signal was observed from the H + (CH$_3$)$_3$COCl reaction. Tests of the differential rate law showed first-order dependence of the HCl emission intensity on [H] and [(CH$_3$)$_3$COCl] for concentration ranges of $2-19 \times 10^{12}$ cm^{-3}. Comparison of the HCl emission intensity with those of the H + Cl$_2$ reaction gave a rate constant for HCl($v \geq 0$) formation

Observation of OCS Infrared Chemiluminescence

J. Phys. Chem. A, Vol. 104, No. 47, 2000 **11019**

TABLE 2: Summary of Results for H + RC(O)SCl

reactant	rate constant[a] (cm³ s⁻¹)	[HCl]:[OCS]	$\langle E_v(HCl)\rangle^e$ (kcal mol⁻¹)	$\langle E_v(OCS)\rangle^d$ (kcal mol⁻¹)
CH₃OC(O)SCl	$3.0 \pm 1.0 \times 10^{-12}$	$9.9 \pm 3.6\ (9.0)^d$	12.6	$15.7\ (14.6)^d$
ClC(O)SCl	$\approx 1.0 \times 10^{-12\ b}$	$7.6 \pm 2.1\ (6.1)^d$	9.5	$9.7\ (8.4)^d$
FC(O)SCl	$\sim 1.2 \times 10^{-12\ b}$	$4.8 \pm 0.9\ (4.4)^d$	12.7	$18.6\ (17.2)^d$
	$\sim 0.54 \times 10^{-12\ c}$	$2.5 \pm 0.9^c\ (2.3)^d$	17.6^c	
(CH₃)₃COCl	$1.5 \pm 0.2 \times 10^{-11}$		12.7	

[a] Rate constant for formation of HCl($v \geq 0$). [b] These rate constants have an uncertainty of a factor of 2 because of the weak signals. [c] For HF($v \geq 0$) formation. [d] These entries include only the emitting levels of OCS. Estimates (see text) for the contributions of the six nonemitting levels to the OCS concentration give the numbers in parentheses. [e] For HCl($v \geq 0$) and HF($v \geq 0$); see Table 3 for the distributions and the text for the estimation of P_0.

TABLE 3: Summary of Thermochemistry[a] and the HCl(v) and HF(v) Distributions from the H + RC(O)SCl Reactions

reactant	product	ΔH_0^{oa} (kcal mol⁻¹)	P_0	P_1	P_2	P_3	P_4
CH₃OC(O)SCl	→ CH₃OC(O)S + HCl	−43	25 ± 4	25 ± 4	24 ± 3	17 ± 2	9 ± 2
	→ CH₃O + OCS + HCl	−26					
	→ CH₃OH + OCS + Cl	−28					
ClC(O)SCl	→ ClC(O)S + HCl	−44	38 ± 5	29 ± 5	18 ± 3	9 ± 2	6 ± 2
	→ Cl + OCS + HCl	−46					
FC(O)SCl	→ FC(O)S + HCl	−43	25 ± 5	25 ± 5	23 ± 3	17 ± 2	10 ± 2
	→ F + OCS + HCl	−12					
	→ Cl + OCS + HF	−40	23 ± 5	26 ± 5	27 ± 4	15 ± 3	9 ± 2
(CH₃)₃COCl	→ (CH₃)₃CO + HCl	−55	15 ± 3	32 ± 3	38 ± 2	13 ± 2	2 ± 1

The header for the distribution columns reads: HC(v) or HF(v) distribution

[a] The available energy is usually defined as $\langle E \rangle = \Delta H_0^o + E_a + 4.5RT$. Since the uncertainty in ΔH_0^o is comparable to the thermal energy and the E_a is unknown, we just used the ΔH_0^o values as the available energy.

of $(1.5 \pm 0.2) \times 10^{-11}$ cm³ s⁻¹; the P_0 value was taken as $0.5P_1$. These experiments were much easier than for the RC(O)SCl molecules, because the (CH₃)₃COCl rate constant is an order of magnitude larger, with a correspondingly higher HCl(v) emission intensity.

III.B. Vibrational Distributions. *III.B.1. CH₃OC(O)SCl.* Collisions with hydrogen atoms are the principal relaxation process for HCl(v) in the flow reactor,[14,15,19,25] and the best distribution was determined from spectra obtained at the lowest combination of [H] and Δt for [CH₃OC(O)SCl] $\leq 8.0 \times 10^{12}$ cm⁻³. The average HCl($v = 1-4$) distribution from 14 independent spectra was 33 ± 4:32 ± 4:23 ± 2:12 ± 2. These experiments included a set with constant [H] = 7.0 or 8.0 × 10¹² cm⁻³ and variable [CH₃OC(O)SCl] from 0.7 to 8.0 × 10¹² cm⁻³; the HCl($v = 1-4$) distribution was invariant. The reaction time, Δt, was 0.22 or 0.24 ms. The measured HCl($v \geq 1$) distribution for H + Cl₂ for the same [H] and approximately equivalent [Cl₂] was 12:39:40:9, which matches the accepted nascent distribution[14,15] to within the combined uncertainties. This comparison shows that relaxation from the [H] was not important and the HCl(v) distribution from H + CH₃OC(O)SCl should be the nascent distribution. Since the nascent HCl($v \geq 1$) distribution from reaction 1 is rather flat, we set $P_0 = P_1$. This distribution, which is given in Table 3, corresponds to $\langle E_v(HCl)\rangle = 12.6$ kcal mol⁻¹.

The HCl spectrum in Figure 1 shows the presence of high rotational lines, up to $J = 25$ in the P branch, and the R branch bandheads were also observed. These features were consistently observed from experiments with pressure ≤ 0.6 Torr, while at higher pressures only emission from the Boltzmann component was observed. From averaging over several experiments, the population in the high J component ($J = 10-25$) represented 5^{+4}_{-2}% of the total HCl($v \geq 1$) distribution. It seems likely[21] that the nascent HCl(v) distribution had a much higher population for $J \geq 10$, and the reaction must release considerable rotational energy to the HCl(v) product.

A representative OCS spectrum and the corresponding box distribution from CH₃OC(O)SCl are shown in Figure 3B,C. The

distribution declines with E_v, but it extends to ~13000 cm⁻¹ (37 kcal mol⁻¹) and gives $\langle E_v(OCS)\rangle = 15.7$ kcal mol⁻¹. The relative contribution from the box corresponding to the six lowest levels was estimated as 0.1 and the global $\langle E_v(OCS)\rangle$ becomes 14.6 kcal mol⁻¹, which is just slightly larger than $\langle E_v(HCl)\rangle$. As discussed previously, $\langle E_v(OCS)\rangle$ was invariant for a change in Ar pressure of a factor of 2 for $\Delta t = 0.3$ ms. The OCS spectrum also was independent of [CH₃OC(O)SCl] from 0.7 to 8.0×10^{12} cm⁻³. We believe that the $\langle E_v(OCS)\rangle$ should be close to the nascent vibrational energy.

After the box distribution for OCS is assigned, the relative concentrations of HCl and OCS can be estimated from the experimental I_{HCl}/I_{OCS} intensity ratio of 2.3 ± 0.9. As noted in section III.A.1, this ratio corresponds to [HCl]/[OCS] = 9.0. The "average" Einstein coefficient for OCS is ~5 times larger than for HCl and, irrespective of the simulation model chosen for OCS, the [HCl] is greater than the [OCS].

A few experiments were done with the D + CH₃OC(O)SCl reaction. The DCl emission was not very useful, because it was weak and partly overlapped by the OCS emission. The OCS band, however, was strong and matched that obtained from H + CH₃OC(O)SCl, which provides confirmation of the $\langle E_v(OCS)\rangle$ given in Table 2.

III.B.2. ClC(O)SCl. Experiments with the lowest [H] and Δt gave a HCl(v) distribution of $P_1-P_4 = 47:28:15:10$. The HCl(v) spectrum from H + Cl₂ under similar conditions was nearly nascent, and this HCl(v) distribution should be close to the nascent distribution. Since the vibrational distribution declines with increasing v, P_0 was set equal to $1.3P_1$ and the P_0-P_4 distribution is 38:29:18:9:6, which gives $\langle E_v(HCl)\rangle = 9.5$ kcal mol⁻¹. The HCl(v) distributions were invariant for [ClC(O)SCl] = $8.0-16.0 \times 10^{12}$ and $\Delta t = 0.15-0.25$ ms; however, increasing [H] from 0.8 to 3.0×10^{13} cm⁻³ gave some relaxation. High rotational lines of HCl($v = 1,2$) were not observed for any conditions from the ClC(O)SCl reaction. The absence of the high rotational levels and the lower $\langle E_v(HCl)\rangle$, relative to the CH₃OC(O)SCl reaction, suggests that interaction
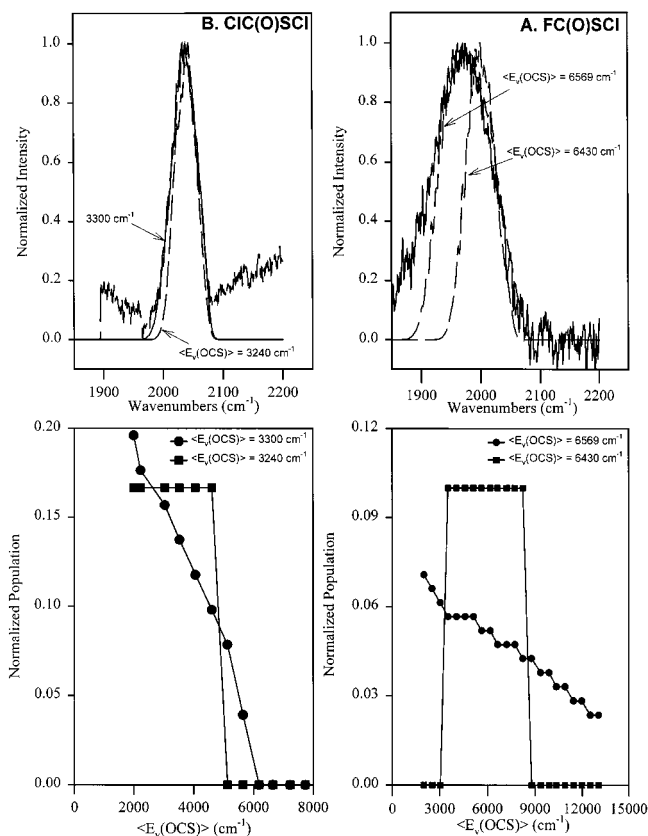
Figure 6. Comparison of the experimental and simulated $\Delta v_3 = -1$ OCS emission spectra for the (A) H + FC(O)SCl and (B) H + ClC-(O)SCl reactions. The vibrational energy distributions for each reaction are shown in the lower panels; in each case the flat distribution gives the narrower emission spectrum.

with the C−Cl bond contributes to HCl formation, as well as the interaction with the S−Cl bond.

The OCS spectrum from ClC(O)SCl is much narrower and shifted to higher wavenumbers than the spectra from either CH₃OC(O)SCl or FC(O)SCl; compare Figure 6B to Figures 3B and 6A. The OCS distribution does not extend beyond 6000 cm⁻¹ (17 kcal mol⁻¹), and it has higher populations in the first few boxes than for the other two reactions. A flat distribution also could be used to simulate the spectrum from ClC(O)SCl, but we chose the same shape as for the CH₃OC(O)SCl reaction. The $\langle E_v(OCS)\rangle$ of the emitting levels is 9.7 kcal mol⁻¹; the contribution from the six nonemitting levels was set as 25%, which reduces $\langle E_v(OCS)\rangle$ to 8.4 kcal mol⁻¹. Within their combined uncertainties, $\langle E_v(OCS)\rangle$ is equal to $\langle E_v(HCl)\rangle$.

III.B.3. FC(O)SCl. The presence of the HF(v) and HCl(v) emissions demonstrates that reaction can occur with halogens at both the carbon and sulfur atoms. From limited data due to restriction on the available sample, the average HF(vs) distribution was $P_1-P_4 = 33 \pm 3{:}35 \pm 5{:}20 \pm 3{:}12 \pm 3$, while the average HCl($v$) distribution was $P_1-P_4 = 35 \pm 3{:}31 \pm 2{:}21 \pm 2{:}13 \pm 2$. The HF and HCl distributions were investigated over a moderate range of [H] = 2.0−4.0 × 10¹³ cm⁻³, [FC(O)SCl] = 6.0−11.0 × 10¹² cm⁻³ for Δt = 0.3 ms. In general, HF(v) distributions are less affected by high [H] than are HCl(v) distributions[25] and the HF(v) distribution should be close to the nascent distribution. However, the HCl(v) distribution, P_1-P_4 = 25:43:27:5, from H + Cl₂ for these conditions was somewhat relaxed. The [H] was slightly larger than for the best conditions used for the ClC(O)SCl reaction, and apparently the difference was enough to cause observable relaxation from the strongly inverted HCl(v) from H + Cl₂. It is also possible that [H] >

0.5 [H₂] or Δt > 0.3 ms. For the purpose of calculating the $\langle E_v(HF)\rangle$ and $\langle E_v(HCl)\rangle$ in Table 2, we assumed $P_0(HF)$ = $0.9P_1(HF)$ and $P_0(HCl)$ = $P_1(HCl)$. These distributions correspond to $\langle E_v(HCl)\rangle$ = 12.7 and $\langle E_v(HF)\rangle$ = 17.6 kcal mol⁻¹. These $\langle E_v\rangle$ are considered lower limits; however, relaxation will affect a flat distribution to a lesser degree than the HCl(v) distribution from H + Cl₂.
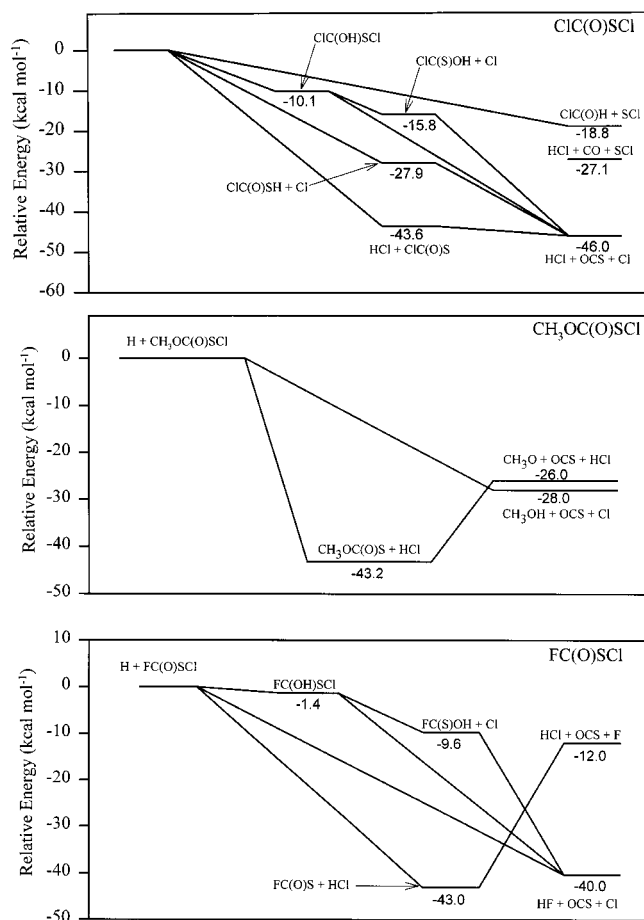
The OCS spectra from the FC(O)SCl reaction were the most difficult to analyze, because the spectra extended closer to the cutoff limit of the detector, indicating a high $\langle E_v(OCS)\rangle$. Although the distribution extends to higher E_v, the shape of the distribution is similar to that of the CH₃OC(O)SCl reaction, compare Figures 6A (lower panel) and 3C. A flat distribution is not suitable for the FC(O)SCl reaction as shown in Figure 6A. Extrapolation suggests that ∼10% of the distribution could be in the six nonemitting levels, and the $\langle E_v(OCS)\rangle$ is lowered from 18.6 to 17.2 kcal mol⁻¹. Since some relaxation may have occurred based on the H + Cl₂ experiment, the $\langle E_v(OCS)\rangle$, $\langle E_v(HF)\rangle$, and $\langle E_v(HCl)\rangle$ values are considered to be lower limits. Nevertheless $\langle E_v(OCS)\rangle$ is larger than $\langle E_v(HCl)\rangle$ and comparable to $\langle E_v(HF)\rangle$. Although the OCS band appears very strong in Figure 1, adjustment for the Einstein coefficients gives a smaller OCS yield than for HF or HCl, and the global [HF]/[OCS] and [HCl]/[OCS] ratios are 2.5 and 4.8, respectively.

III.B.4. (CH₃)₃COCl. The average P_1-P_4 distribution from seven experiments at low [H] and short Δt was 38 ± 4:45 ± 2:15 ± 2:2 ± 1. This distribution showed no dependence on [(CH₃)₃COCl] from 4−19 × 10¹² cm⁻³. The vibrational distribution from H + Cl₂ for the same experimental condition was nascent[15a] and the HCl(v) distribution should be reliable. The P_0 contribution was set as 0.5P_1 and the overall P_0-P_4 distribution becomes 15 ± 3:32 ± 3:38 ± 8:13 ± 2:2 ± 1 with $\langle E_v(HCl)\rangle$ = 12.7 kcal mol⁻¹. The H + CF₃OCl reaction[15a] had a similar, but more sharply peaked, distribution with P_1-P_4 = 23:47:26:4.

IV. Discussion

IV.A. Thermochemistry. The available energy for the H + RC(O)SCl reactions cannot be calculated in the usual way because the $\Delta H_f^o(RC(O)SCl)$ values have not been reported. Our attempt to estimate the available energies for these reactions is summarized in the Appendix; the results are tabulated in Table 3 and shown in Figure 7. Two available energies are listed in Table 3 for formation of HCl: the first corresponds to removal of the Cl atom from the sulfur site, and the second is for HCl formation with dissociation of the RC(O)S radical. These radicals can be bound by a few kcal mol⁻¹ and the overall $\Delta H°$ for formation of OCS + R + HCl can be less than for reaction 1a. Even if the subsequent dissociation of the RC(O)S radicals is exoergic, the energy available to HCl formed by direct abstraction will be released in the first step. According to our calculation, the C(O)SCl radical is not bound, and formation of HF from FC(O)SCl has only one entry in Table 3. Formation of HCl from the carbon site of ClC(O)SCl has the same $\Delta H°$ as the second entry (HCl + OCS + Cl) in Table 3, but the mechanism is different from reaction at the sulfur site. The expectation of a weakly bound RC(O)S radical is supported by the ab initio calculations for FC(O)S (31 kcal mol⁻¹) and CH₃OC(O)S (17 kcal mol⁻¹), but not for ClC(O)S. The latter did have a stable structure and apparently a potential energy barrier exists for exoergic dissociation to Cl + OCS. Although the calculations may overestimate the difference between the dissociation energies of FC(O)S and ClC(O)S, a similar trend was reported for $D(Cl−CO_2)$ vs $D(F−CO_2)$.[26]

Observation of OCS Infrared Chemiluminescence

J. Phys. Chem. A, Vol. 104, No. 47, 2000 **11021**

Figure 7. Schematic representation of the calculated energetics for the carbonylsulfenyl reactions (see Appendix for details). No attempt was made to identify intermediate species for the CH$_3$OC(O)SCl + H system, except for the CH$_3$OC(O)S radical. The energy of a third set of possible products (HF + CO + SCl) lies 25 kcal mol^{-1} below H + FC(O)SCl in the bottom panel.

The ΔH_f^o values for (CH$_3$)$_3$CO, −21.7 kcal mol^{-1}, and (CH$_3$)$_3$COCl, −40 kcal mol^{-1}, have been reported.[27] Based on these values, the available energy for the H + *tert*-butyl hypochlorite reaction is ≈56 mol^{-1}. The ΔH_f^o((CH$_3$)$_3$COCl), which is based upon liquid-phase photoinitiated calorimetry[27] and may not be very reliable, gives D_{298}((CH$_3$)$_3$CO−Cl) = 47.6 kcal mol^{-1}. Within the experimental uncertainties, the available energies for the CF$_3$OCl[15b] and (CH$_3$)$_3$COCl reactions are the same, and we will use 55 kcal mol^{-1} as the available energy for both cases.

IV.B. Mechanisms. *IV.B.1. (CH$_3$)$_3$COCl.* For an available energy of 55 kcal mol^{-1}, the HCl(v) distribution of Table 3 corresponds to a fractional vibrational energy ($\langle f_v(HCl)\rangle = \langle E_v(HCl)\rangle/\langle E_{available}\rangle$) of 0.23, which is smaller than for CF$_3$OCl (0.28)[15b] and Cl$_2$O (0.32).[14] The shape of the HCl(v) distribution is similar to the other abstraction reactions, but the $v = 3$ and 4 populations are slightly smaller than for CF$_3$OCl. As expected for direct halogen atom abstraction reactions by H atoms, the HCl(v) distributions do not extend to the thermochemical limit.[14,15] The *tert*-butoxy radical readily dissociates to acetone and CH$_3$,[28] and the *tert*-butoxy radical may store some vibrational energy as it relaxes from the equilibrium (CH$_3$)$_3$COCl geometry to the (CH$_3$)$_3$CO structure. The available evidence supports a direct Cl abstraction mechanism, but with some special dynamics associated with the *tert*-butyl group. It is interesting that the rate constants for the CF$_3$OCl and (CH$_3$)$_3$-COCl reactions are nearly the same.

IV.B.2. RC(O)SCl Molecules. The arguments below suggest that the event associated with HCl formation from reaction at the sulfur site is not responsible for formation of the vibrationally excited OCS molecules.

(1) A set of experiments in which F atoms were reacted with thioacetic acid, CH$_3$C(O)SH, gave very strong HF emission plus weak OCS emission from only *low* vibrational levels.[23] The estimated [OCS]-to-[HF] ratio from the interaction of F atoms with just the S−H bond was 1:20. Even in this favorable case, hydrogen abstraction followed by dissociation of CH$_3$C(O)S to give OCS with 10−12 kcal mol^{-1} of vibrational energy does not occur.

(2) If the calculated ΔH^o_{rxn} values are correct for FC(O)SCl and CH$_3$OC(O)SCl, the available energy is much too small for both HCl and OCS to be excited to the levels cited in Table 3 for reactions 1a and 1b. Furthermore, a potential energy barrier probably exists for dissociation of these RC(O)S· radicals, thus requiring even more energy.

(3) The OCS yield is consistently much smaller than the HCl yield. The total rate constant associated with loss of [H] seems to be larger than the rate constant for just HCl formation, and other reaction pathways exist. However, the experimental data for the latter claim are based only on the ClC(O)SCl reaction.

(4) The observation of HF from FC(O)SCl shows that the H atom can interact with a halogen attached to either carbon or sulfur. Direct attack by H atoms on C−Cl or C−F bonds usually has a large activation energy, and the HF formation presumably proceeds by H atom addition followed by unimolecular rearrangement from one or more intermediates.

(5) The ab initio calculations predict that the RC(O)S radicals are bound, whereas the C(O)SCl radical is dissociative.

For these reasons, we will discuss the reaction mechanism as an interaction with the S−Cl site that can be either direct or proceed by an intermediate, RC(O)SCl·H. The RC(O)SCl·H intermediate subsequently can dissociate to HCl and RC(O)S or it can rearrange to give RH + OCSCl; the OCSCl radical will dissociate to OCS + Cl. The ab initio D(Cl−SC(O)R) values are all similar, and the available energy for formation of HCl from the sulfur site is essentially the same for the three reactions. In our opinion, the most likely sites for H atom addition to the RC(O)SCl molecules is the O or S atom. Addition of an H atom to the carbon site would generate an oxygen-centered radical that would subsequently dissociate by rupture of the C−S bond to give a stable aldehyde.[29a] A theoretical study[29b] of H + F$_2$CO favored addition of the H atom to the oxygen site, but the activation energy was ∼15 kcal mol^{-1}; the FC(OH)F radical decomposes by dissociation back to H + F$_2$CO or by HF elimination, with the latter having the higher threshold energy. We attempted to generate HCl emission from reacting H atoms with CH$_3$C(O)Cl in our flow reactor, but no emission was observed and an activation energy exists for both abstraction and addition. Given the small rate constants for the primary H + RC(O)SCl reactions and the low yield of OCS relative to HCl, the generation of some OCS from a secondary reaction of H with the RC(O)S radicals cannot be excluded, even though we found no experimental evidence for a second-order dependence of the [OCS] yield on [H].

The CH$_3$OC(O)SCl reaction favors HCl over OCS by a factor of 9. For an available energy of 43 kcal mol^{-1}, $\langle f_v(HCl)\rangle \approx$ 0.3, which is consistent with the H atom reactions with the inorganic sulfur chlorides (SCl$_2$, SOCl$_2$, S$_2$Cl$_2$), although those reactions gave more inverted HCl(v) distributions.[13] Of special note is the release of high rotational energy to the HCl($v = 1$, 2) product, which also was observed for the H + SCl$_2$ reaction.[13]

The high rotational energy was associated with a mechanism involving H addition to the sulfur atom followed by migration of the H to the chlorine atom with high angular momentum being acquired in the migratory motion. By analogy, identification of a highly rotationally excited HCl($v = 1, 2$) distribution suggests the addition of H to the sulfur atom in the CH$_3$OC-(O)SCl reaction. The OCS product had an average vibrational energy of ~15 kcal mol^{-1}. If we associate OCS formation with the CH$_3$OH + OCS + Cl channel with ≈28 kcal mol^{-1} of available energy, $\langle f_V(OCS) \rangle = 0.52$. The mechanism could be four-centered elimination from the intermediate formed by H atom addition to the sulfur atom, and the dynamics may resemble the more completely characterized formation of CH$_4$ + CO$_2$ from the unimolecular decomposition of acetic acid, which had $\langle f_V(CO_2) \rangle = 0.32$.[3]

The HCl(v) distribution from FC(O)SCl corresponds to $\langle f_V(HCl) \rangle = 0.29$ for an available energy of 43 kcal mol^{-1}. The channel involving HF formation gives $\langle f_V(HF) \rangle = 0.44$ and $\langle f_V(OCS) \rangle = 0.43$ for an available energy of 40 kcal mol^{-1}. These values seem rather high, but the available energy probably has been underestimated. A higher $\langle f_V(OCS) \rangle$, relative to the CH$_3$OC(O)SCl reaction, is plausible due to the smaller number of vibrational modes in FC(O)SCl·H. The ab initio calculations also identified a bound FC(S)OH intermediate, but formation of HF + OCS from this intermediate would provide even less available energy. The more serious problem with the proposed mechanism is the 2-fold larger yield of HF relative to OCS. Some possible reasons for the *apparent* low yield of OCS could be uncertainty in the intensity measurements, e.g., failure to record emission below the detection limit or underestimation of the concentration of the OCS($v_3 = 0$) molecules by the simulations model or because of incorrect Einstein coefficients for the high energy OCS molecules. Although reservation should be maintained about the mechanism, other plausible processes, e.g., the FC(S)OH intermediate or the H + FC(O)S secondary reaction, also would give [HF] ≈ [OCS]. The available energy from formation of HFCO + SCl seems too low for subsequent HF elimination from HFCO to be important.

The fraction of the energy released to HCl (0.21) and OCS (0.19) from ClC(O)SCl is the lowest of the three reactions. The energy available to HCl by direct abstraction from the sulfur site is similar for all three reactions, and the lower $\langle f_V(HCl) \rangle$ from ClC(O)SCl probably reflects a contribution to the HCl(v) yield by formation of HCl from the chlorine atom on the carbon center. Possible explanations for the low $\langle E_V(OCS) \rangle$ might be a role for other intermediates in OCS formation, such as ClC(S)OH or ClC(O)SH, which were identified in ab initio calculations, or dissociation of some of the ClC(O)S radicals.

V. Conclusions

The major objective of this project was to evaluate the utility of the OCS($\Delta v_3 = -1$) infrared chemiluminescence as a probe of state-resolved reaction dynamics. The emission is relatively easy to detect since the Einstein coefficient is large and the $\Delta v_3 = -1$ band lies in a sensitive region of the InSb detector. Unlike CO$_2$, excitation in the bending mode of OCS cannot be distinguished from v_3 excitation, and only the total vibrational energy can be assigned from computer simulation of the $\Delta v_3 = -1$ spectra. Short times (≤0.3 ms) and low pressures (≤0.6 Torr of Ar) must be used to avoid vibrational relaxation in a flow reactor experiment.

The H + RC(O)SCl reactions seem to occur by two pathways. One involves interaction with the S−Cl end of the molecule to give HCl with $\langle f_V(HCl) \rangle \approx 0.3$. The $\langle f_V(OCS) \rangle$ values were 0.52,

0.43, and 0.19 for the CH$_3$OC(O)SCl, FC(O)SCl, and ClC(O)-SCl reactions, respectively. The second pathway involves addition, reaction 2a, probably at the sulfur atom, followed by unimolecular decomposition, reactions 2b.3 + 2c, giving HR + OCS (+Cl). Ab initio calculations were employed to estimate the reaction exergicity and hence $\Delta H°_f(RC(O)SCl)$. Interpretations for the mechanism for OCS formation depend, in part, upon the bond dissociation energy for the R−C(O)S radicals, and experimental verification of the thermochemistry of these interesting radicals is needed. We have argued that the dissociation of R−C(O)S is *not* the major pathway for formation of OCS in the H + RC(O)SCl systems, rather OCS arises from dissociation of OCS−Cl. Although we favor the addition mechanism, eq 2a followed by eqs 2b.3 + 2c, for the formation of OCS, a contribution from the H + RC(O)S secondary reaction cannot be totally excluded. Analogy to the unimolecular dissociation of the H−C(O)−ONO and CH$_3$−C(O)−ONO molecules formed by HCO and CH$_3$CO reacting with NO$_2$ is interesting.[5,30] In this case, dissociation to give NO and HC-(O)O, or CH$_3$C(O)O, is followed by rupture of the H, or CH$_3$, with formation of vibrationally excited CO$_2$ molecules that are observed by infrared chemiluminescence.

The H + (CH$_3$)$_3$COCl reaction was investigated as a reference system involving direct Cl atom abstraction from a large molecule. The $\langle f_V(HCl) \rangle = 0.23$ is somewhat lower than for chlorine atom abstraction from smaller molecules containing the S−Cl or O−Cl bond. The rate constant for (CH$_3$)$_3$COCl was 1 order of magnitude larger than for the carbonylsulfenyl molecules, which have rate constants of 1−3 × 10^{-12} cm^3 s^{-1} for HCl formation.

Appendix

The S−Cl bond dissociation energies for SCl$_2$, S$_2$Cl$_2$, and S(O)Cl$_2$ have been reported as 45, 46, and 54 kcal mol^{-1}, respectively, from the highest observed vibrational energy of the XeCl(B) and HgCl(B) products from the reactions of Xe(6s[3/2]$_2$) and Hg(6s6p,^{3}P$_0$) atoms with these molecules.[31] A similar approach was attempted for ClC(O)SCl and CH$_3$OC-(O)SCl using the metastable Xe atom reactions, e.g.:

$$Xe(6s[3/2]_2) + ClC(O)SCl \rightarrow XeCl(B) + ClC(O)S \quad (A-1)$$
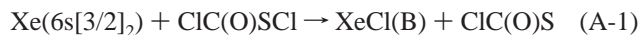
The XeCl(B−X) emission was strong and the spectra gave the same upper limit for D(S−Cl) of 64 ± 2 kcal mol^{-1} for each molecule. This value may be too large, but this experiment suggests that these bonds are stronger than those of the inorganic sulfur halides. Reactions of H atoms with R−S−Cl compounds typically give $\langle f_V(HCl) \rangle \approx 0.3$ and the highest HCl(v,J) level does not extend to the thermochemical limit.[13,14] Thus, observation of HCl($v = 4$), which gives D(S−Cl) ≤ 70 kcal mol^{-1}, does not provide a useful estimate for the bond energies of the RC(O)S−Cl molecules.

Experimental D(R−C(O)S) values would be useful, because the $\Delta H°_f(OCS)$ and $\Delta H°_f(R)$ values are known[32] and then the $\Delta H_f°(RC(O)S)$ could be evaluated. The HCO$_2$ and HC(O)S radicals have been studied. The most recently measured D(H−CO$_2$)[33] value is −13 ± 3 kcal mol^{-1}, which agrees with the result that can be obtained from the thermochemistry of HC(O)OH and D(HC(O)O−H).[32] The ab initio calculated values

Observation of OCS Infrared Chemiluminescence

J. Phys. Chem. A, Vol. 104, No. 47, 2000 **11023**

for $D(H-CO_2)$[34] are approximately 0 kcal mol^{-1}, and the calculated $D(H-COS)$[35] is 8.1 kcal mol^{-1}. According to the calculations, both radicals have significant barriers, 10−20 kcal mol^{-1}, for dissociation. Experiments[16] in which HCO_2 and HOCO are generated by the F + HC(O)OH reaction suggest that HCO_2 dissociates whereas HOCO does not. In our laboratory, we investigated the F + HCOOD reaction in the flow reactor and searched for CO_2 emission without success. In fact, the thermochemistry for stepwise formation of DF + (CO_2 + H) is unfavorable for observation of $\Delta\nu_3 = -1$ infrared emission from CO_2. We can conclude that H−CO_2 and H−C(O)S are, at best, weakly bound but that small barriers may exist for their dissociation.

The CH_3-CO_2, F−CO_2, and Cl−CO_2 radicals also have been examined. Since $D_{298}(CH_3C(O)O-H)$ and $\Delta H^o_f(CH_3C(O)OH)$ are established, $\Delta H^o_f(CH_3-CO_2) = -50$ kcal mol^{-1} is reliable and $D_{298}(CH_3-CO_2) = -10$ kcal mol^{-1} can be accepted.[32] This is in accord with the observation[36a] that the decomposition of methyl acetate to give CH_3 and CH_3CO_2 is followed by the dissociation of CH_3-CO_2. The decomposition of CH_3-CO_2 also has been observed from the reaction of $CH_3C(O)$ with NO_2, which proceeds by association followed by dissociation of $CH_3C(O)O-NO$.[30,36b] The $D(CH_3-C(O)S)$ can be estimated from the S−H bond dissociation energy of $CH_3C(O)SH$ and the $\Delta H_f^o(OCS)$ and $\Delta H_f^o(CH_3)$.[32] For $\Delta H^o_{f,298}(CH_3C(O)SH) = -39.7$ and $D_{298}(H-SC(O)CH_3) = 93$ kcal mol^{-1}, the dissociation of $CH_3C(O)S$ is thermoneutral. Similar arguments[31d] from dimethyl carbonate, $CH_3OC(O)OCH_3$, suggest that $D(CH_3O-C(O)O)$ is approximately 0 kcal mol^{-1}. According to the ab initio results,[26] $D(Cl-CO_2)$ and $D(F-CO_2)$ are −30 and 5 kcal mol^{-1}, respectively. This summary suggests that RC(O)S radicals may have comparable or slightly higher binding energies than RCO_2 radicals; however, the actual energy change in the dissociation step should be small.

Since the experimental data were limited, we used the Gaussian 92 ab initio package[37] to calculate optimized geometries and total energies for the main species of interest (reactants, products, and RC(O)S radicals). The geometry of each species was first optimized at the UHF (unrestricted Hartree−Fock) and MP2 (second-order Moller−Plesset perturbation theory) levels with a 6-31G* basis set. The optimized geometries were used for single-point calculations at the MP4 (fourth-order Moller−Plesset perturbation theory) level with the 6-311G** basis set to obtain the energies and vibrational frequencies for all three reactions. Additional optimizations, total energy calculations, and vibrational frequency calculations were performed at the MP2 level with the larger 6-311++G** basis set for intermediate species of the ClC(O)SCl and $CH_3OC(O)$-SCl reaction. In all cases, an energy difference was calculated relative to stable products (e.g. H + $CH_3OC(O)SCl$ vs CH_3O + OCS + HCl) and adjustments were made for zero point energies. The calculated results were summarized in Figure 7.

At the MP2/6-311++G** level, the calculated energy change for HCl + $CH_3OC(O)S$ is 43.2 kcal mol^{-1} and the calculated $D(CH_3OC(O)S-Cl)$ is 51.6 kcal mol^{-1}. If the experimental $D(H-Cl) = 102.2$ kcal mol^{-1} is combined with the calculated energy difference, the derived $D(CH_3OC(O)S-Cl)$ is 59 kcal mol^{-1}, which is close to the value obtained from the Xe(6s) experiment. The value based on the experimental $D(H-Cl)$ is presumed to be more accurate than the value from the ab initio $D(H-Cl)$ because the latter is too low by 7.6 kcal mol^{-1}. The dissociation of $CH_3OC(O)S$ to OCS + CH_3O was calculated to be 16.7 kcal mol^{-1} endoergic. Even if this value is too large, the calculation suggests that $CH_3OC(O)S$ is bound. The

calculated difference between CH_3O + OCS + HCl and CH_3OH + OCS + Cl is 1.3 kcal mol^{-1}, which matches the experimental difference of 2 kcal mol^{-1}. On the basis of the energy difference calculated with the 6-311++G** basis sets and the energy for the CH_3O + OCS + HCl limit, we recommend $\Delta H^o_f(CH_3OC(O)SCl) = -76$ kcal mol^{-1}; the uncertainly is expected to be between 5 and 10 kcal mol^{-1}.

The calculated structure and vibrational frequencies for ClC(O)SCl were in agreement with the experimentally measured structure[38] and vibrational frequencies.[39] The calculated energy difference, 46 kcal mol^{-1}, between HCl + OCS + Cl and H + ClC(O)SCl using the 6-311++G** basis set gave $\Delta H^o_{f,298}(ClC(O)SCl) = -32$ kcal mol^{-1}. The calculated S−Cl bond energy is 51 kcal mol^{-1}, but using the experimental $D(HCl)$ and the 43 kcal mol^{-1} energy difference between H + ClC(O)SCl and HCl + ClC(O)S gives $D(ClC(O)S-Cl) = 59$ kcal mol^{-1}. Searches were made for several intermediates, and bound structures were found for the radical corresponding to the addition of H atoms to oxygen, ClC(OH)SCl, the ClC(S)OH molecule from Cl displacement, and the thiol counterpart, ClC(O)SH. The ClC(O)S radical had a stable structure, but the dissociation is 2.4 kcal mol^{-1} exoergic. The reaction rate for Cl + OCS is quite slow,[40] as expected since ClC(O)S and OCSCl are not stable radicals.

The calculated structure of FC(O)SCl is in agreement with the experimentally determined geometry.[41] According to the results from the 6-31G** basis set, $\Delta H^o_f(FC(O)SCl) = -77$ and $D(FC(O)S-Cl) = 52$ kcal mol^{-1}. The calculated energy differences between HCl + OCS + F and two other sets of products, HF + CO + SCl and HF + OCS + Cl, were −13.0 and −28.3 kcal mol^{-1}, respectively, which are within 5 kcal mol^{-1} of the experimental values, −17.6 and −33.0 kcal mol^{-1}, respectively.

References and Notes

(1) Polyani, J. C. *Angew. Chem., Int. Ed. Engl.* **1987**, *26*, 952.

(2) Agrawalla, B. S.; Setser, D. W. In *Gas-Phase Chemiluminescence and Chemi-Ionization*; Fontijn, A., Ed.; Elsevier: Amsterdam, 1985.

(3) (a) Boutkovskaya, N. I.; Manke, G. C., II; Setser, D. W. *J. Phys. Chem.* **1995**, *99*, 11115. (b) Nguyen, M. T.; Sengupta, D.; Raspoet, G.; Vanquickenborne, L. G. *J. Phys. Chem.* **1995**, *99*, 11883.

(4) Butkovskaya, N. I.; Setser, D. W. *J. Chem. Phys.* **1996**, *105*, 8064; **1998**, *108*, 2434.

(5) Boutkovskaya, N. I.; Setser, D. W. *J. Phys. Chem.* **1998**, *102*, 9715.

(6) Boutkovskaya, N. I.; Muravyov, A. A.; Setser, D. W. *Chem. Phys. Lett.* **1997**, *266*, 223.

(7) (a) Arunan, E.; Manke, G. C., II; Setser, D. W. *Chem. Phys. Lett.* **1993**, *207*, 81. (b) Arunan, E.; Setser, D. W. *J. Phys. Chem.* **1991**, *95*, 4190.

(8) (a) Kagann, R. H. *J. Mol. Spectrosc.* **1982**, *94*, 192. (b) Belafhal, A.; Fayt, A.; Guelachvili, G. *J. Mol. Spectrosc.* **1995**, *174*, 1.

(9) Fayt, A.; Vandenhaute, R.; Lahaye, J. G. *J. Mol. Spectrosc.* **1986**, *119*, 233.

(10) (a) Flynn, G. W. *Acc. Chem. Res.* **1981**, *14*, 334. (b) Mandich, M. L.; Flynn, G. W. *J. Phys. Chem.* **1980**, *73*, 1265. (c) Mandich, M. L.; Flynn, G. W. *J. Chem. Phys.* **1980**, *73*, 3679. (d) Siebert, D. R.; Flynn, G. W. *J. Chem. Phys.* **1976**, *64*, 4973.

(11) (a) Zittel, P. F. *J. Phys. Chem.* **1991**, *95*, 6802. (b) Zittel, P. F.; Sedam, M. A. *J. Phys. Chem.* **1990**, *94*, 5801. (c) Zittel, P. F.; Sedam, M. A. *Chem. Phys. Lett.* **1988**, *148*, 486.

(12) Hudgens, J. W.; Gleaves, J. T.; McDonald, J. D. *J. Chem. Phys.* **1976**, *64*, 2528.

(13) (a) Sung, J. P.; Setser, D. W. *Chem. Phys. Lett.* **1978**, *58*, 98. (b) Wickramaaratchi, M. A.; Setser, D. W.; Hildebrandt, B.; Korbitzer, B.; Heydtmann, H. *Chem. Phys.* **1984**, *84*, 105.

(14) Wategaonkar, S. J.; Setser, D. W. *J. Chem. Phys.* **1989**, *90*, 251, 6223.

(15) (a) Rengarajan, R.; Setser, D. W.; DesMarteau, D. D. *J. Phys. Chem.* **1994**, *98*, 10568. (b) The available energy for the H + CF_3OCl reaction was erroneously listed as 51 kcal mol^{-1} rather than 55 kcal mol^{-1}.

(16) Ruscic, B.; Schwartz, M.; Berkowitz, J. *Chem. Phys.* **1989**, *91*, 6780.

(17) Arunan, E.; Rengarajan, R.; Setser, D. W. *Can. J. Chem.* **1994**, *72*, 568.

(18) Seakins, P. W.; Woodbrdige, E. L.; Leone, S. R. *J. Phys. Chem.* **1993**, *97*, 5633.

(19) Arunan, E.; Wategaonkar, S. J.; Setser, D. W. *J. Phys. Chem.* **1991**, *95*, 1539.

(20) Haas, A.; Reinke, H. *Angew. Chem., Int. Ed.* **1967**, *6*, 705.

(21) Sung, J. P.; Malins, R. J.; Setser, D. W. *J. Phys. Chem.* **1979**, *83*, 1007.

(22) Arunan, E.; Setser, D. W.; Oglive, J. F. *J. Chem. Phys.* **1992**, *97*, 1734.

(23) Manke, G. C., II. Ph.D. Thesis, Kansas State University, 1998.

(24) (a) Atkinson, R.; Baulch, D. L.; Cox, R. A.; Hampson, R. F.; Kerr, J. A.; Troe, J. *J. Phys. Chem. Ref. Data* **1992**, *21*, 1125. (b) Dobis, O.; Benson, S.-W. *J. Phys. Chem. A* **2000**, *104*, 777. This reference reports $(0.46 \pm 0.04) \times 10^{-11}$ cm^3 s^{-1} for the room-temperature rate constant of H + Cl$_2$, which is a factor of 2 lower than the recommended value in ref 24a.

(25) Leone, S. R. *J. Phys. Chem. Ref. Data* **1982**, *11*, 953.

(26) Francisco, J. S.; Goldstein, A. N. *Chem. Phys.* **1988**, *127*, 73.

(27) Walling, C.; Papaioannou, C. G. *J. Phys. Chem.* **1968**, *72*, 2260.

(28) Fittschen, C.; Hippler, H.; Viskolz, B. *Phys. Chem. Chem. Phys.* **2000**, *2*, 1677.

(29) (a) Wang, B.; Hou, H.; Gu, Y. *J. Phys. Chem.* **1999**, *103*, 5075. (b) Zachariah, M. R.; Tsang, W.; Westmoreland, P. R.; Burgess, D. R. F., Jr. *J. Phys. Chem.* **1995**, *99*, 12512.

(30) Butovskaya, N. I.; Setser, D. W. *J. Phys. Chem. A* **2000**, *104*, in press.

(31) (a) Kolts, J. H.; Velazco, J. E.; Setser, D. W. *J. Chem. Phys.* **1979**, *71*, 1247. (b) Zhang, F. M.; Oba, D.; Setser, D. W. *J. Phys. Chem.* **1987**, *95*, 1099.

(32) (a) Chase, M. W., Jr.; Davies, C. A.; Downey, J. R., Jr.; Frurip, D. J.; McDonald, R. A.; Syverud, A. N. *J. Phys. Chem. Ref. Data* **1995**, *14* (Suppl.)1. (b) Benson, S. W. *Thermochemical Kinetics*; John Wiley & Sons: New York, 1976. (c) McMillen, D. F.; Golden, D. M. *Annu. Rev. Phys. Chem.* **1982**, *33*, 493. (d) Stull, D. R.; Westrum, E. F., Jr.; Sinke, G. C. *The Chemical Thermodynamics of Organic Compounds*; Wiley: New York, 1969.

(33) Kim, E. H.; Bradforth, S. E.; Arnold, D. W.; Metz, R. B.; Neumark, D. M. *J. Chem. Phys.* **1995**, *103*, 7801.

(34) (a) Rauk, A.; Yu, D.; Armstrong, D. A. *J. Am. Chem. Soc.* **1994**, *116*, 8222. (b) Kuda, K.; Schatz, G. C.; Wagner, A. F. *J. Chem. Phys.* **1981**, *95*, 1635. (c) Kuda, K.; Koures, A. G.; Harding, L. B.; Schatz, G. C. *J. Chem. Phys.* **1991**, *96*, 7465.

(35) (a) Rice, B. M.; Pai, S. V.; Chabalowski, C. F. *J. Phys. Chem.* **1998**, *102*, 6950. (b) Rice, B. M.; Chabalowski, C. F. *J. Phys. Chem.* **1994**, *98*, 9488; **1998**, *102*, 3847 (erratum). (c) Rice, B. M.; Cartland, H. E.; Chabalowski, C. F. *Chem. Phys. Lett.* **1993**, *211*, 283.

(36) (a) Hintsa, E. J.; Wodtke, A. M.; Lee, Y. T. *J. Phys. Chem.* **1988**, *92*, 5379. (b) Slagle, I. R.; Gutman, D. *J. Am. Chem. Soc.* **1982**, *104*, 4741.

(37) Frisch, M. J.; Trucks, G. W.; Head-Gordon, J.; Gill, P. M. W.; Wong, M. W.; Andres, J. B.; Raghavachari, K.; Binkley, J. S.; Gonzalez, C.; Martin, R. L.; Fox, D. J.; Defrees, D. J.; Baker, J.; Stewart, J. J. P.; Pople, J. A. *Gaussian 92*, revision G.45; Gaussian Inc.: Pittsburgh, PA, 1992.

(38) So, S. P. *J. Mol. Struct.* **1988**, *168*, 217.

(39) (a) Shen, Q.; Hagen, K. *J. Mol. Struct.* **1985**, *128*, 41. (b) Della Védova, C. O.; Cutin, E. H.; Varetti, E. L.; Aymonino, P. J. *Can. J. Spectrosc.* **1984**, *29*, 69.

(40) Clyne, M. A. A.; MacRobert, J. J.; Murrels, T. P.; Steif, L. J. *J. Chem. Soc., Faraday Trans. 2* **1984**, *80*, 877.

(41) Mack, H. G.; Oberhammer, H.; Della Védova, C. O. *J. Phys. Chem.* **1991**, *95*, 4238.